scientific reports

Check for updates

OPEN

Exploiting long read sequencing to detect azole fungicide resistance mutations in *Pyrenophora teres* using unique molecular identifiers

Katherine G. Zulak[1]✉, Lina Farfan-Caceres[1], Noel L. Knight[1,2] & Francisco J. Lopez-Ruiz[1]

Resistance to fungicides is a global challenge as target proteins under selection can evolve rapidly, reducing fungicide efficacy. To manage resistance, detection technologies must be fast and flexible enough to cope with a rapidly increasing number of mutations. The most important agricultural fungicides are azoles that target the ergosterol biosynthetic enzyme sterol 14α-demethylase (CYP51). Mutations associated with azole resistance in the *Cyp51* promoter and coding sequence can co-occur in the same allele at different positions and codons, increasing the complexity of resistance detection. Resistance mutations arise rapidly and cannot be detected using traditional amplification-based methods if they are not known. To capture the complexity of azole resistance in two net blotch pathogens of barley we used the Oxford Nanopore MinION to sequence the promoter and coding sequence of *Cyp51A*. This approach detected all currently known mutations from biologically complex samples increasing the simplicity of resistance detection as multiple alleles can be profiled in a single assay. With the mobility and decreasing cost of long read sequencing, we demonstrate this approach is broadly applicable for characterizing resistance within known agrochemical target sites.

Fungicides are an important tool for the management of crop disease with the use of demethylase inhibitor or azole fungicides dominating in both agriculture and clinics[1,2]. Azoles are single site systemic fungicides that target the cytochrome P450 sterol 14α-demethylase (CYP51) enzyme, which has an essential role in the biosynthesis of the fungal sterol ergosterol[3]. Azole fungicides disrupt the function of CYP51 and therefore membrane stability and fluidity through a combination of ergosterol depletion and the accumulation of toxic sterol intermediates[4].

Azole fungicides are highly efficient and resistance development is generally slower than other single site fungicides with incomplete cross resistance among members of the class[2,5]. However an increasing number of cases of azole resistance have been reported among economically important crop pathogens such as *Zymoseptoria tritici*[6], *Fusarium graminearum*[7], *Blumeria graminis* spp.[8,9], and *Pyrenophora teres*[10,11]; as well as human fungal pathogens such as *Aspergillus fumigatus*[12]. There are three main mechanisms of azole fungicide resistance; mutations in the *Cyp51* gene that alter fungicide binding, over-expression of *Cyp51* due to promoter modifications, and increased efflux out of the cell[5]. These mechanisms are not mutually exclusive, and several can exist in the same isolate, increasing resistance levels. A further complication is the existence of more than one paralogous *Cyp51* gene in the filamentous Ascomycetes, including many phytopathogens. However, in ascomycetes with more than one *Cyp51* paralogue, mutations associated with fungicide resistance are associated with mainly *Cyp51A*[10,13,14].

P. teres f. *teres* (*Ptt*) and *P. teres* f. *maculata* (*Ptm*) are the causal agents of net form of net blotch and spot form of net blotch of barley (*Hordeum vulgare*) respectively. *Ptt* contains one *Cyp51B* gene and two copies of *Cyp51A*; *Cyp51A1* and *Cyp51A2*, with the fungicide resistance mutation F489L only occurring in *Cyp51A1*[10] and to date no mutations associated with fungicide resistance have been found in *Cyp51B*. Expression of all three genes was induced by tebuconazole but no promoter changes were found[10]. Unlike *Ptt*, *Ptm* contains only one copy of *Cyp51A*, but both promoter and coding sequence mutations are associated with azole fungicide resistance[11]. Solo-long terminal repeat (LTR) insertion elements were present in the *Cyp51A* promoter at five different locations and the F489L mutation was encoded by three different non-synonymous mutations[11]. Isolates containing both insertions and the F489L mutation showed high resistance to azoles, while isolates containing either insertions or F489L had a moderately resistant phenotype[11]. *Ptt* and *Ptm* can also form hybrids in nature[15–19] with one hybrid

[1]Centre for Crop and Disease Management, School of Molecular and Life Sciences, Curtin University, Bentley, WA 6102, Australia. [2]Centre for Crop Health, University of Southern Queensland, Toowoomba, QLD 4350, Australia. ✉email: katherine.zulak@curtin.edu.au

haplotype exhibiting a high level of resistance to azole fungicides suggested to have acquired the trait through natural recombination between the two forms[11,19].

Detection and monitoring of fungicide resistance in both agriculture and clinics is critical for monitoring resistant populations and informing appropriate management. For example, if resistance to an azole compound is detected, chemical management can be adjusted to avoid placing excessive selective pressure on the pathogen population and then the population closely monitored to ensure the treatment change was effective. This requires rapid, accurate and point of care molecular detection technologies capable of capturing the complex network of both known and evolving genetic mutations that cause resistance. Several allele-specific technologies such as loop-mediated isothermal amplification, digital PCR, and quantitative PCR (qPCR) have been deployed for the detection and monitoring of fungicide resistance in phytopathogens[20–25]. Although useful, these technologies suffer from two major limitations, the need for a separate assay for each mutation and the inability to detect new mutations. In *Ptm* there are several different promoter insertions and coding sequence mutations that can exist separately or in combination[10,11]. *Ptm* and *Ptt* are also closely related and can form hybrids[18,19], further complicating resistance diagnoses. Thus, screening for resistance from field samples becomes a complicated and time-consuming process involving a large array of assays. In addition, the F489L mutation is encoded by three codons in *Ptm*[11] which could result in a false negative if these changes were not known.

Amplicon sequencing of marker genes such as 16S ribosomal DNA for prokaryotes and 18S rDNA and internal transcribed spacers (ITS) for eukaryotes has been used in the field of metagenomics to characterize microbial diversity, mainly using high throughput short read sequencing technologies such as Illumina[26]. However, these short read lengths can constrain taxonomic resolution to family or genus level and even confuse taxonomic assignment if different parts of the marker gene are used[27]. Longer read sequencing technologies such as Pacific Biosciences (PacBio) and Oxford Nanopore Technologies (ONT) could remedy this issue but suffer from relatively high error rates and resolving single nucleotide polymorphisms is problematic. PacBio has resolved this issue through circular consensus sequencing to generate high accuracy (99.8%) long reads[28]. Recently, this was exploited to produce error-corrected full length rRNA genes and resolve the majority of a bacterial mock community to species level[29]. This technology was also used recently to characterize azole, succinate dehydrogenase inhibitor (SDHI), and quinone outside inhibitor (QoI) resistance in the phytopathogen *Z. tritici*[30]. Target genes were multiplexed, amplified, and sequenced using PacBio circular consensus sequencing to characterize the range of resistance genotypes present in European populations of *Z. tritici*. The authors also included nine housekeeping genes to further profile the strains present in these populations[30]. This study presents a comprehensive system capable of profiling target genes to three modes of action, however samples must be sent to centralized laboratories to perform sequencing and this method involves culturing individual isolates, both of which can be time consuming.

ONT employs long read technology with the added benefit of portability which enables sequencing on demand that can be done in any laboratory or in the field, an attractive prospect for rapid resistance diagnosis. ONT sequencing was used to profile azole resistant haplotypes in the phytopathogen *Z. tritici*[31]. The authors sequenced mock communities with varying quantities of one to three isolates as well as infected leaves to identify haplotypes associated with azole resistance. To correct sequencing errors, reads were filtered using Filtlong (https://github.com/rrwick/Filtlong) and corrected using Canu[32], which resulted in a per position consensus between 98 and 99%[31]. Recently Ion Torrent, Illumina and ONT sequencing were used alongside pyrosequencing and qPCR to profile cytochrome b mutations in *Plasmopara viticola* single spored isolates and field populations[33]. ONT sequencing was largely consistent with the other techniques, with the added benefit of detection of multiple SNPs within a single cytochrome b gene, something not possible with shorter read technologies or qPCR[33].

Several pipelines have been developed to mitigate the per base 2 to 25% error rate[34] of long read sequencing such as denoising[35,36] and intramolecular-ligated nanopore consensus sequencing[37,38], and recently unique molecular identifiers (UMIs) which tag individual molecules with a UMI sequence containing random bases in a particular pattern which can be used to bioinformatically sort molecules based on their original templates[39]. This method results in a low consensus error rate of 0.0042% and a chimera rate of less than 0.02% when sequenced on an R10.3 flow cell[39]. Chimeras are artifacts which arise when two or more sequences are joined together incorrectly and then further amplified and often occur in complex mixed samples. These artifacts are problematic because they are needlessly sequenced and can affect the perception of the DNA pool. In fact, chimeras can be upwards of 20% of the PCR products in metagenomics studies, depending on polymerase and cycling conditions[40]. The high accuracy and low chimera rate of UMIs make this method ideally suited to single nucleotide polymorphism (SNP)-level detection of both known and new mutations in fungicide target genes in complex biological samples with highly similar sequences.

Here we applied the UMI amplicon sequencing approach to profile both inserts and single nucleotide changes in the azole target gene *Cyp51A* in two forms of *P. teres* and a hybrid. We validated this approach using a mix of currently known haplotypes of *Ptt* and *Ptm* and a hybrid and resolved all variants with 100% identity to reference sequences, although some clusters had erroneous SNPs mostly in mono- and dinucleotide repeat regions. We then optimized a workflow to process diseased leaf samples and profiled their *Cyp51A* haplotypes and validated this using qPCR, resulting in the detection of a point mutation associated with azole resistance in *Ptt*. This method is broadly applicable and can be used not only to profile fungicide target gene mutations, but also to characterize chemical resistance in other kingdoms such as bacteria, plants, insects, and animals.

Results

UMI PCR assay design and sequencing optimisation

To ensure our assay detected all known *Cyp51A* variants to date, five *Ptm,* one *Ptt* and one *Ptm/Ptt* hybrid isolate that represent all currently known *Cyp51A P. teres* haplotypes were selected for amplicon sequencing (Fig. 1,

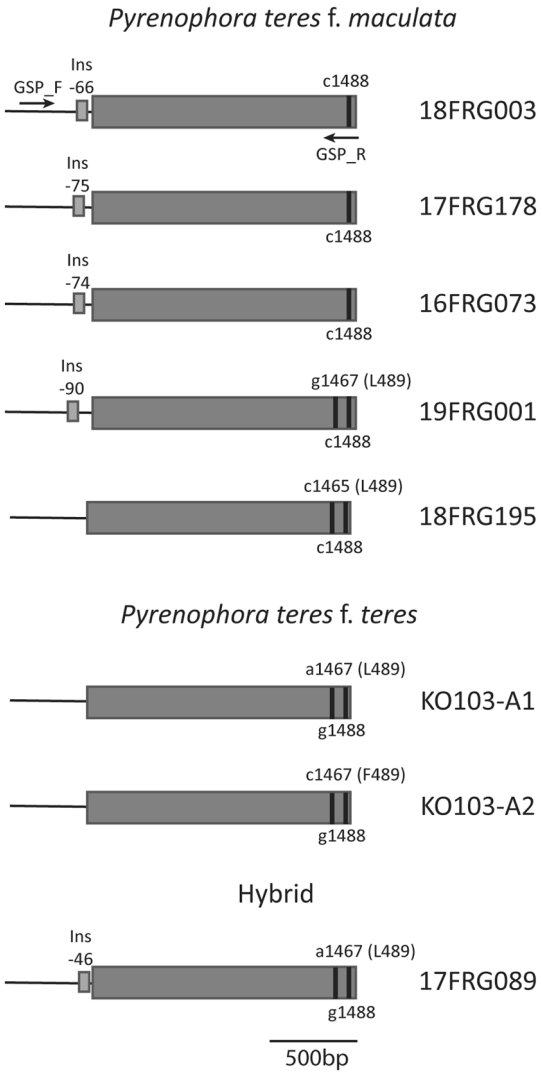

Figure 1. Genotypes of the azole fungicide target gene *Cyp51* in seven isolates of *Pyrenophora teres* f. *maculata*, *P. teres* f. *teres* and a hybrid amplified and sequenced in this study. Arrows indicate approximate primer positions and vertical black lines indicate nucleic acid positions associated with *P. teres* form differentiation and mutations associated with azole fungicide resistance (L489) and sensitivity (F489). *Ins* = promoter insertion associated with azole fungicide resistance.

Isolate ID	Year	Form	Location	Resistance phenotype	Reference	Genbank accession promoter	Genbank accession CDS
KO103	2013	*Ptt*	Kojonup, WA	MR	Mair et al.[10]		KX578217.1
16FRG073	2016	*Ptm*	Gibson, WA	MR	Mair et al.[11]	MT499783.1	ON534218.1
17FRG178	2017	*Ptm*	Coomalbidgup, WA	MR	Mair et al.[11]	MT499784.1	MT499777.1
18FRG003	2018	*Ptm*	Munglinup, WA	MR	Mair et al.[11]	MT499785.1	ON534219.1
18FRG195	2019	*Ptm*	Pithara, WA	MR	Mair et al.[11]		MT499777.1
19FRG001	2019	*Ptm*	Broomehill, WA	HR	Mair et al.[11]	MT499787.1	MT499780.1
17FRG089	2017	*Ptm*/*Ptt* hybrid	Takaralup, WA	HR	Turo et al.[19], Mair et al.[11]	MT499786.1	MT499779.1

Table 1. Isolates used in this study. *Ptt Pyrenophora teres* f. *teres*, *Ptm Pyrenophora teres* f. *maculata*, *MR* moderately resistant, *HR* highly resistant, *CDS* coding sequence.

Table 1). We aligned the promoter and coding sequences of the seven isolates and designed gene-specific primers to capture all known promoter inserts, the F489L mutations and the g1448c SNP that discriminates *Ptt* from *Ptm* and the hybrid (Fig. 1, Table 2). This resulted in an amplicon that captured all known mutations related with azole resistance in *P. teres*. Primers were validated on genomic DNA from individual isolates and resulted in bands of the expected sizes (18FRG003, 17FRG178, 16FRG073, 19FRG001 and 17FRG089 = 2327 bp; 18FRG195 = 2193 bp; KO103-A1 = 2191 bp; KO103-A2 = 2201 bp).

For the *Cyp51A* mock community sequencing, we determined the optimal amount of input DNA to be 1.3 ng by empirically testing sequencing runs using 10, 5, 3 and 1.3 ng of gDNA from each of the seven isolates pooled into one PCR reaction (Table 1) and found the pipeline yielded sufficiently high cluster densities with 1.3 ng of

Name	Isolate	Description	Sequence	Publication
GSP_F	All	Forward gene specific primer UMI PCR1	CAAGCAGAAGACGGCATACGA GAT NNNYRNNNYRNNNYRNNN GCTCGCGTTGGTTGTAGC	Gene specific primer—this study UMI and UVP – Karst et al. 2021
GSP_R	All	Reverse gene specific primer UMI PCR1	AATGATACGGCGACCACCGAG ATC NNNYRNNNTRNNNYRNNN TTACCGCCTCTCCCAGCA	Gene specific primer—this study UMI and UVP – Karst et al. 2021
UVP_F	All	Forward universal primer UMI PCR2	CAAGCAGAAGACGGCATACGA GAT	Karst et al. 2021
UVP_R	All	Reverse universal primer UMI PCR2	AATGATACGGCGACCACCGAG ATC	Karst et al. 2021
Ptt_R1ID1_F3	KO103	Forward primer Ptt species identification	GACGCGGCTAATGTCGTAA	Knight et al. 2023
Ptt_R1ID1_B3_R		Reverse primer Ptt species identification	GGCGGTAACAGCACCAAG	Knight et al. 2023
Ptt_R1ID1_P		Probe Ptt species identification	AATCGGCGGACCGTCAGGAT	Knight et al. 2023
Ptm_r5ID12_F3.2	18FRG003 17FRG178 16FRG073 19FRG001 18FRG195	Forward primer Ptm species identification	GTTGGCTGACTTGTGTAGACAC	Knight et al. 2023
Ptm_r5ID12_B3_R		Reverse primer Ptm species identification	AAACGCCCTTTAGCAGTCTT	Knight et al. 2023
Ptm_r5ID12_P		Probe Ptm species identification	CGCTTGCGCGCATGTTCATT	Knight et al. 2023
PtTi-1_F	16FRG073	Forward primer insertion at –74 bp in *Cyp51A* promoter	AGAACTGTGTCCAAAAGTAGA GTGTC	Knight et al. 2023
Pt_CYP51A_ promoter_R		Reverse primer insertion at –74, -46, -75, -66 and -90 bp in *Cyp51A* promoter	GGAGAGATGGGCGTAGAACA	Knight et al. 2023
PtTi-1_P		Probe insertion at –74 bp in *Cyp51A* promoter	TGTCCTACATCCGACATAGAG AACCATTTC	Knight et al. 2023
PtTi-2_F	17FRG089	Forward primer insertion at –46 bp in *Cyp51A* promoter	TCATCCTATCGACTTGCTTTA TGTC	Knight et al. 2023
PtTi-2_P		Probe insertion at –46 bp in *Cyp51A* promoter	TACCTCTGTCCTACATCCGAC ACTTTACTG	Knight et al. 2023
PtTi-3_F	17FRG178	Forward primer insertion at –75 bp in *Cyp51A* promoter	CTAAGAACTGTGTCCAAAAGT AGATGTC	Knight et al. 2023
PtTi-3_P		Probe insertion at –75 bp in *Cyp51A* promoter	TGTCCTACATCTGACAGTAGA GAACCATTTC	Knight et al. 2023
PtTi-4_F	18FRG003	Forward primer insertion at –46 bp in *Cyp51A* promoter	TCCAAAAGTAGAGAACCATTT TGTC	Knight et al. 2023
PtTi-4_P		Probe insertion at –66 bp in *Cyp51A* promoter	TCCTACATCCGACACATTTCA CCCTAT	Knight et al. 2023
PtTi-5_F	19FRG001	Forward primer insertion at –90 bp in *Cyp51A* promoter	ACCCTGACGCTAAGAACTTGTC	Knight et al. 2023
PtTi-5_P		Probe insertion at –90 bp in *Cyp51A* promoter	TCCTACATCTGACAGAACTGT GTCCAAA	Knight et al. 2023
CYP51_mm2L_ L489-1_F	KO103-A1 17FRG089 Field samples	Forward primer a1467 (L489) in *Cyp51A*	GTACCGACTATAGCACCA AGTT + A	Knight et al. 2023
CYP51A1_ F-L489_R		Reverse primer a1467/c1465 (L489) in *Cyp51A*	GCCTCTCCCAGCAAATCT	Knight et al. 2023
CYP51A1_mm1_ L489-1_P		Probe a1467 (L489) in *Cyp51A*	CTCTAGGGGGCGCGA + TAAC	Knight et al. 2023
CYP51_mm2L_ L489-3_F	18FRG195	Forward primer c1465 (L489) in *Cyp51A*	GTACCGACTATAGCACAATG + C	Knight et al. 2023
CYP51A1_mm1_ L489-3_P		Probe c1465 (L489) in *Cyp51A*	CTAGGGGGCGCGAGA + GCAT	Knight et al. 2023
CYP51_F489_mm2L_F	Field samples	Forward primer c1467 (F489) in *Cyp51A*	GTACCGACTATAGCACCA AGTT + C	Knight et al. 2023
CYP51_F489_mm1_P	Field samples	Probe c1467 (F489) in *Cyp51A*	GCCTCTCCCAGCAAATCT	Knight et al. 2023

Table 2. Primers used in this study.

gDNA from each isolate but not with the higher starting concentrations. PCR reactions using less than 1.3 ng template DNA per isolate failed to yield product.

ONT sequencing of mock community resolves all variants

We sequenced the amplicons from the seven isolate mock community using the MinION, which resulted in 2,164,642 passed sequences. To determine the minimum number of reads per target for cluster formation and variant calling, we inputted a randomly sub-sampled set of 1.5 M, 1 M, 750 K, 500 K and 250 K reads from the original dataset into the longread UMI pipeline (Fig. 2, Table 3). The pipeline failed using 250 K reads, but outputted variants using ≥ 500 K sequences (Fig. 2, Table 3). The 500 K read input failed to identify three haplotypes, whereas the ≥ 750 K read inputs resolved all haplotypes (Fig. 2, Table 3). Although equimolar amounts of each isolate were used as input into the UMI PCR reaction, we did not observe equal cluster densities (Fig. 2).

Variants with cluster depth of > 100 were 100% identical to the reference sequences and differentiated between a one base pair shift in the promoter insert (Supplemental Fig. S1). However, with increasing sequence input we noticed a concomitant increase in spurious clusters with either deletions or base changes (Table 4). All spurious clusters analysed in this study contained errors in the *Cyp51A* coding sequence, with the majority consisting of base pair deletions in a heteropolymer a/g di-nucleotide region (Fig. 3). Even though the number of spurious clusters increased with the number of input sequences, the depth of the spurious clusters was approximately an order of magnitude less than the variants which were 100% identical to the reference sequences, thus easily

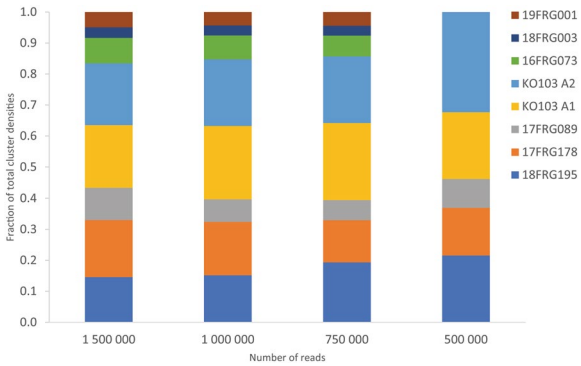

Figure 2. Cluster densities of each *Cyp51A* allele as a fraction of the total for 1,500,000, 1,000,000, 750,000 and 500,000 randomly sampled reads inputted into the longread UMI bioinformatic pipeline.

Number of reads	Cluster depth for each *Cyp51A* variant							
	18FRG195	17FRG178	17FRG089	KO103 A1	KO103 A2	16FRG073	18FRG003	19FRG001
1,500,000	1465	1854	1037	2030	2008	830	342	494
1,000,000	395	450	189	615	560	201	84	113
750,000	135	95	45	173	150	47	22	31
500,000	14	10	6	14	21	0	0	0
250,000	0	0	0	0	0	0	0	0

Table 3. Number of subsampled reads versus depth of clusters with 100% identity to the respective reference *Cyp51* sequences for each variant in a mock community.

Number of reads	Number spurious clusters for each *Cyp51A* variant (cluster depth)							
	18FRG195	17FRG178	17FRG089	KO103 A1	KO103 A2	16FRG073	18FRG003	19FRG001
1,500,000	2 (5, 5)	2 (3, 5)	1 (4)	1 (5)	2 (6, 5)	1 (7)	0	0
1,000,000	0	0	1 (4)	2 (3, 3)	1 (4)	0	0	0
750,000	0	1 (3)	0	0	0	0	0	0
500,000	0	0	0	0	0	0	0	0
250,000	0	0	0	0	0	0	0	0

Table 4. Number of spurious clusters and depth with < 100% identity to respective reference *Cyp51* sequences for each variant for mock community.

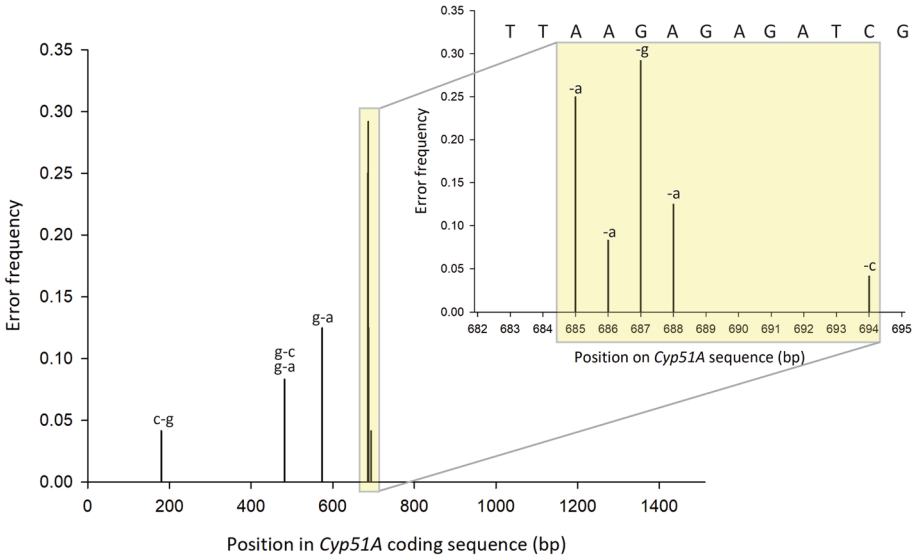

Figure 3. Frequency, type, and position in *Cyp51A* coding sequence of errors present in all spurious variant clusters observed in this study.

discarded (Tables 3, 4). We determined that approximately 100 K reads per haplotype was optimal for resolution of all haplotypes and reduction in spurious clusters, while maximizing the number of samples that can be run on each flow cell. We determined the average error rate of all variant consensus sequences to be 0.03% and did not observe any chimeras.

To validate the mutations in the *Cyp51A* mock community, we analysed the input DNA used for ONT sequencing with qPCR assays specifically designed to detect the genetic changes in each haplotype (Knight et al.[25]; Fig. 1, Table 2) with the pure genomic DNA from each isolate as positive controls (Supplemental Table S1). Negative controls consisted of genomic DNA from an isolate known to not contain the mutation being tested. The qPCR analysis confirmed the presence of each expected mutation associated with fungicide resistance in the seven isolates tested (Supplemental Table S1).

Custom workflow identifies Cyp51 haplotype associated with azole resistance from field samples

To avoid lengthy isolation procedures to generate single spore isolates, we developed a customized workflow designed for complex cultures from leaf samples (Fig. 4). Since these are field collected samples, it is not possible to determine if mutations originated from one or more different isolates without isolating single spores. We analysed five barley leaf samples from South Australia with net form of net blotch symptoms. Since the leaf samples were confirmed using qPCR to contain only *Ptt* (Supplementary Table S2), two clusters representing *Cyp51A1* and *Cyp51A2* were expected, as there are two *Cyp51A* alleles in *Ptt*[10]. The resulting total of 845,625 passed sequences as well as 750 K, 500 K, 375 K, 300 K, 250 K and 100 K randomly sampled sequences were inputted into the longread UMI pipeline. No variants resulted from either the 100 K or 250 K read inputs, however 300 K reads and above successfully generated variants (Table 5). Like the mock community analysis, spurious clusters increased with increasing read inputs (Tables 4, 5). Errors found in spurious clusters were like those found in the mock community analyses (Fig. 3) except for an adenine to cytosine substitution in a homopolymer region eight nucleotides before the start codon in one spurious cluster (Supplemental Fig. S2), but these were of discernibly low depth and thus easily discarded (Table 5). In all successful pipeline runs, two high-depth clusters resulted with two non-synonymous and one synonymous mutation in the coding region and two promoter SNPs (Supplemental Fig. S2). We re-evaluated the reads/haplotype to be approximately 100 K to 150 K reads/haplotype for haplotype detection and minimization of spurious clusters (Table 5). The two non-synonymous coding-region SNPs caused I133V and F489L amino acid substitutions in one of the clusters, the former has been found in both sensitive and resistant *Ptt* isolates and the latter associated with *P. teres* azole resistance[10]. The c1465t substitution causing the F489L mutation was validated as the only mutation present in the five samples by qPCR (Supplementary Table S2).

Discussion

In this study we used the MinION, a portable hand-held sequencer from Oxford Nanopore Technologies, to sequence the azole target gene *Cyp51* from characterized mock communities and net blotch infected leaf samples from a paddock in South Australia. As a proof of concept, we amplified the promoter and coding region of *Cyp51A* from seven isolates representing a diverse array of haplotypes including promoter insertions and coding sequence SNPs from *Ptt*, *Ptm* and a hybrid. The long read UMI pipeline developed by Karst et al., 2021 resolved all insertions and SNPs of all variants with 100% identity to the respective reference *Cyp51A* sequences. Our method also discriminates between *Ptt* and *Ptm* as the nucleotide at position 1488 in the *Cyp51A* gene is a

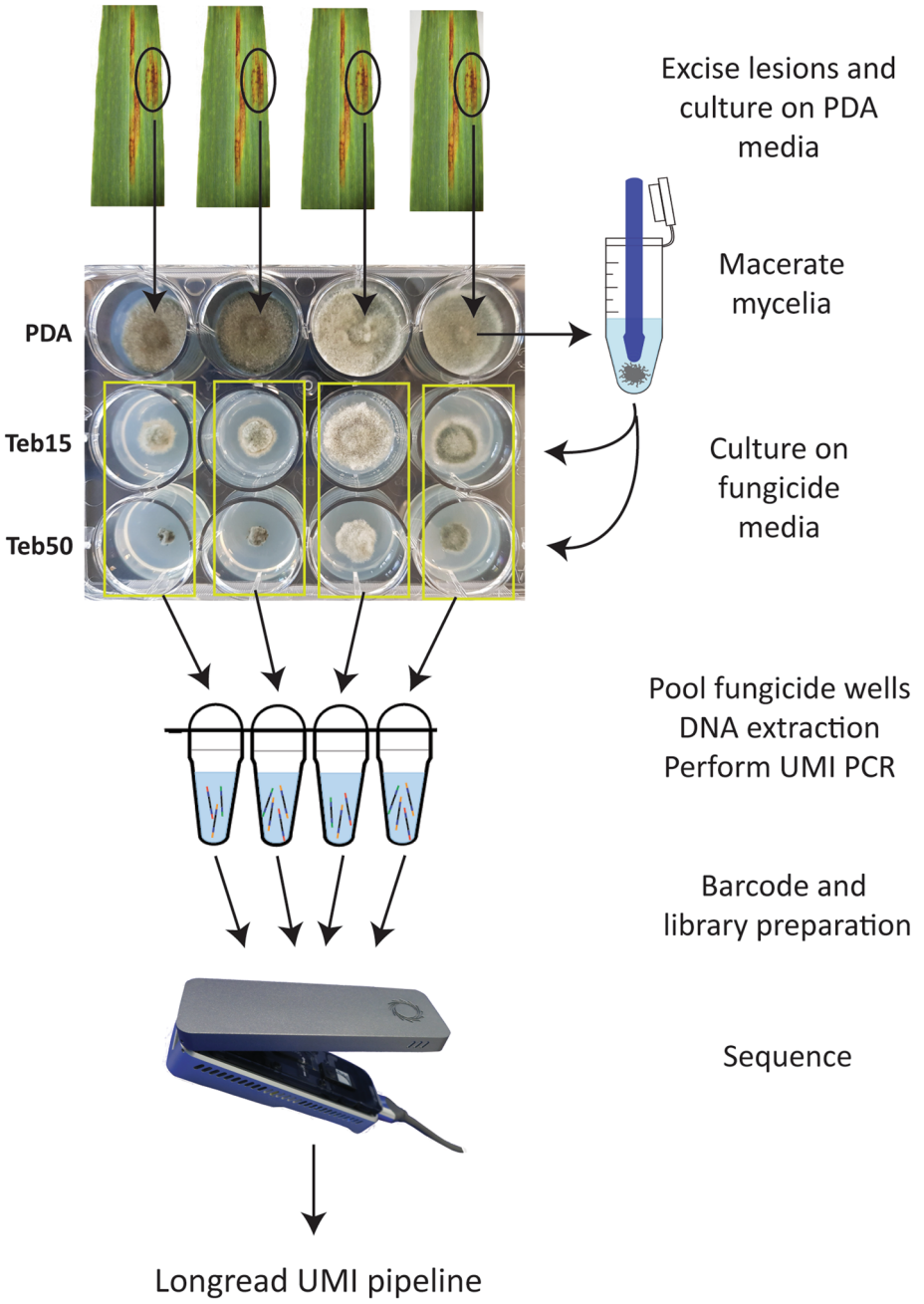

Figure 4. Workflow for culturing, amplification, sequencing, and bioinformatic analysis of mycelia cultured on tebuconazole amended media from infected leaf samples. Teb15 = 15 µg mL^{-1}; Teb50 = 50 µg mL^{-1}.

	Variant 1 (*Cyp51A1*)		Variant 2 (*Cyp51A2*)	
Number of reads	Depth of true clusters	Number of spurious clusters (depth)	Depth of true clusters	Number of spurious clusters (depth)
750,000	653	5 (9, 3, 4, 6, 3)	781	2 (5, 3)
500,000	118	1 (3)	119	0
375,000	20	0	21	0
300,000	4	0	5	0
250,000	0	n/a	0	n/a

Table 5. Number of subsampled reads versus true cluster depth and number of spurious clusters and associated cluster depth for each variant (*Cyp51A1* and *Cyp51A2*).

cytosine in *Ptm* and a guanine in *Ptt* in all isolates we have sequenced to date. Thus, with one sequencing assay it was possible to determine the *P. teres* form(s) present and associated azole fungicide resistance status. This complex resistance landscape dictates the need to profile the entire target gene and promoter region to resolve the haplotype present, not individual mutations in isolation. This is especially important when profiling biologically complex field samples.

We applied our pipeline to infected barley leaf samples and used a culturing method on fungicide media developed by Knight, et al.[25]. This method has three main advantages: (i) bulking of fungal mycelia for PCR, (ii) removal of plant DNA, and (iii) selection of only fungicide resistant isolates. As expected, we recovered two high depth clusters for each field sample (*Cyp51A1* and *Cyp51A2*), one of which had two non-synonymous SNPs, I133V and F489L, the latter correlates with decreased fungicide sensitivity, while the former does not[10]. The codon which gave rise to the F489L mutation was c1465t which was originally reported in *Ptm*[11] but only recently in *Ptt*[25]. If this codon change had not been discovered prior, the result of an allele-specific assay would have been a false negative, highlighting the utility of our assay for comprehensive resistance profiling. Since our assay provides full sequence information on both promoter and coding sequence mutations, it can decern that F489L and one other coding sequence mutation (I133V) were present, and no promoter insertions were detected to potentially account for the growth in media amended with tebuconazole. To reach this conclusion using traditional methods would involve lengthy single spore culturing procedures and Sanger sequencing, which demonstrates the utility of our assay to deliver several critical pieces of information at once which saves time and cost.

Our assay offers distinct advantages over detection methods such as LAMP and qPCR, especially in field samples where several mutations can co-occur in one allele and several alleles likely are present in one sample. This is especially salient for pathogens without existing target gene mutation profiles, as individual mutation detection assays do not need to be developed. Also, fungal genomes are relatively large compared to viral or bacterial genomes and can be prohibitively expensive to sequence for diagnostic purposes. Amplicon sequencing targets only those genes of interest, therefore reducing the amount of data that needs to be collected and therefore cost of the assay. However, the target gene sequence must be known and if resistance is not solely due to target gene changes it will still be missed.

ONT sequencing was used to profile *Cyp51* mutations in *Z. tritici* mixed isolate mock communities and infected wheat leaves[31]. To mitigate sequencing errors, the authors employed a filtering and correcting approach using Filtlong and Canu, respectively. The filtering step was used to increase the overall quality of the basecalls to the highest quality 10 million bases, however this resulted in read loss when sequenced with the R9.4 MinION flow cell for a Phred score of 13.8 when sequencing *Cyp51* mock communities. It is important to highlight that these issues will likely decrease with increasing accuracy of the R10.4/Kit 14 flow cells and associated chemistry, which has enabled near perfect bacterial genomes without short read or reference polishing[41]. Nevertheless, the authors obtained a per position consensus of 98 to 99% after read correction and identified a total of 16 unique haplotypes of *Z. tritici* across the 16 wheat leaves sampled[31].

Recently, ONT sequencing was used alongside pyrosequencing, qPCR, Ion Torrent, and Illumina sequencing to profile cytochrome b in single spored isolates and field populations of *Plasmopara viticola*, a pathogen of grapes[33]. The use of multiple technologies alongside biological assays allowed the authors to produce a comparative analysis highlighting the advantages and limitations of each. Unlike other sequencing technologies, ONT sequencing detected multiple SNPs in one gene from mixed field samples; however, the main drawback was sequencing errors[33]. The ONT assay had a sensitivity limit of 5% based on detection of unexpected variants[33]. Only reads greater than Q7 were used in the analysis and 5000 reads from each sample were aligned to the reference sequence and variable regions searched using either BLAST or Nanopolish analysis. This study also used a quality score cutoff of 7. Frequency of each variant was computed as percentage of total reads[33].

The use of UMIs for read correction differs from these approaches in several respects. Consensus is determined first at the individual molecule level which results in an error rate of 0.03% using R10.3 flow cell and since two UMIs are required for binning, we found no chimeric sequences. When using the ONT R10.3 flow cell to sequence microbial mock communities, Karst et al. reported an error rate of 0.0042% and a chimera rate of < 0.02%[39]. The chimera filtering function of the UMI pipeline removed 4.8% of chimeric UMI bins[39], highlighting the ability of this pipeline to eliminate these potentially erroneous results. Low error rate and chimera filtering are two important considerations when accurately detecting particularly low abundance variants in complex samples containing similar sequences. Although we did detect approximately 100X lower depth clusters which were not 100% identical, these errors were mostly in homopolymer regions, which is a feature of ONT sequencing, and were easily discarded.

Amplicon sequencing was also used to sequence the target genes of azole, SDHI and QoI fungicides along with several genes used for phylogenetic classification in the phytopathogen *Z. tritici*[30] using PacBio sequencing. PacBio sequencing also suffers from relative high error rates of around 13%[39], however the Sequel platform (Pacific Biosciences, Menlo Park CA, United States) overcomes this by utilizing circular consensus sequencing which resulted in a Phred quality score above Q20 or 99% accuracy[30]. Single spored isolates were generated and tagged using a two-step PCR approach where the first PCR introduced a 'heel' sequence which was then tagged in the second PCR to enable differentiation of each isolate in downstream data analysis[30]. The amount and diversity of data generated in this assay is commendable and is useful for generating both resistance and phylogenetic profiles of isolates in large populations. Our approach differs in that we used UMIs to tag and differentiate individual molecules in complex mixed samples that contain more than one isolate, therefore eliminating the need for isolation of individual strains. Thus, we can potentially detect the full suite of resistance haplotypes present in a lesion without the need for isolations and with SNP-level accuracy due to the generation of molecule-specific consensus sequences.

Our method also exploits the portability of the MinION sequencer, which has the potential to enable diagnostics in the paddock. The MARPLE disease diagnostic and surveillance tool has been recently reported to identify

and assign strains of *Puccinia striiformis* f. sp. *tritici* to distinct lineages with a single sequencing assay using the MinION[42]. Similar to the current study, genetically distinct regions were identified and selectively amplified. The authors comment that the addition of fungicide target genes such as *Cyp51* and the four succinate dehydrogenase subunits would be useful in real time monitoring of known mutations in these genes. It is important to accurately characterize SNP level changes to discover new uncharacterized mutations which would require very high accuracy sequencing techniques. The UMI approach outlined in this study offers higher accuracy and lower chimera rates than previously possible on long read sequencing platforms such as the MinION[39].

We found systemic errors in clusters mostly occurring around single and di-nucleotide repeats in the *Cyp51* gene. These systemic homopolymer-associated errors are a feature of ONT sequencing and were also identified in standard microbial community profiling using UMIs and the ONT platform, mostly as deletions in long cytosine and guanine homopolymers and guanine insertions in non-homopolymer regions[39,43]. Although this phenomenon did result in more clusters than were expected, this was not deemed to be problematic as the clusters could easily be discarded due to their relatively small (approximately 100X lower) cluster depth and majority of errors occurring in one region of the sequence.

Another important factor in the success of the UMI approach is input DNA amount which must be optimised to achieve the desired single molecule coverage and sequencing yield required[39]. We determined the optimal amount of input DNA to be 1.3 ng, but also empirically tested amounts lower and higher than this and found DNA amounts less than 1.3 ng did not yield product while amounts higher than 1.3 ng did not yield sufficient read depth for the UMI consensus sequences. If this method is to be applied directly to infected leaf samples, an intermediate qPCR step would likely be required to determine the amount of pathogen DNA present in the leaf sample, as we found this to be a critical factor to the success of this method.

The DNA used as input for the first PCR reaction in the *Cyp51A* mock community consisted of an equimolar amount of each of the seven *P. teres* isolates, however we did not observe an equal cluster density for each of the true variants. Karst et al. also observed a discrepancy between the theoretical relative abundance of the rRNA operons from the mock community supplied by the manufacturer and the observed relative abundances when sequenced using the UMI pipeline[39]. The authors hypothesized this could be due to biased fragments size, difference in growth rates and primer mismatches. We do not expect these issues to be relevant here as equimolar amounts of genomic DNA were added to the PCR reaction, the amplicons are of similar size and there should theoretically be no primer mismatches among the targets. It is interesting to note that the cluster densities for KO103A1 and KO103A2 were nearly identical, which is expected since the two alleles are from the same isolate. It is possible that the observed differences are isolate dependent. Compounds such as oxidized polyphenols and polysaccharides are known to interfere with PCR[44] and genomic DNA isolations from *P. teres* have been reported to be viscous and discoloured, which required a partial digestion of the cell wall to obtain high quality DNA for PacBio sequencing[45]. We have anecdotally observed differences in pigmentation and viscosity of DNA extractions from different isolates of *P. teres*, and this could potentially cause differential amplification when they are mixed.

While the UMI sequencing approach allows entire gene variants to be described, it currently lacks the precise quantification of allele frequencies. This suggests that quantitative platforms such as qPCR or digital PCR are still complementary for the detection process, especially as they are sensitive and able to detect fungicide resistance mutations as low as 0.2%[22]. Also, our current field sample pipeline relies on a lengthy culturing step for selective growth of resistant isolates, similar to detection pipelines using qPCR or digital PCR[25]. Ideally improvements will be devised which would allow DNA to be extracted directly from diseased leaves for UMI sequencing and amplicon diversity assessments.

In this study, we adapted a UMI PCR-based sequencing method to characterize SNP-level mutations in the azole fungicide target gene *Cyp51*, illustrating the broad applicability of this approach. To improve the sample to result timeline, we are currently trialling direct *Cyp51* SNP detection from infected leaf samples which would eliminate the culturing step. It is also expected that the amount of data required for accurate consensus sequence generation and homopolymer associated errors will decrease with increasing accuracy of ONT sequencing[41]. These improvements would result in a decrease in the per sample sequencing cost, as more samples could be analysed per flow cell. Our approach could also be expanded to include phylogenetically relevant genes for simultaneous lineage profiling as highlighted in previous studies, although this would reduce the data yield for fungicide target genes and therefore the number of samples that can be included in a single run. This method could also be applied to other agrochemical resistance systems such as herbicides, insecticides, and bactericides where accurate and rapid SNP level detection of new mutations is critical.

Materials and methods

Isolate selection and culturing

Seven *P. teres* isolates used in this study are listed in Table 1 and Fig. 1. The details of all isolates have been previously published[10,11]. A single conidium was isolated, grown and stored at − 80 °C as in Mair et al.[10]. Mycelial plugs were then grown on V8 potato-dextrose agar (PDA; 10 g potato-dextrose agar, 3 g CaCO3, 15 g agar, 150 mL V8 juice in 850 mL sterile deionized H_2O) plates and incubated at room temperature in the dark for five to seven days.

Primer design

Cyp51A promoter and coding sequences from *Ptt*, *Ptm*, and hybrid isolates used in this study were aligned with the *Ptt* and *Ptm* reference isolates W1 and SG1, respectively (GenBank accessions for seven isolates listed in Table 1; W1 = KX578221.1 and KX578220.1; SG1 = MT499781.1 and MT499776.1). Conserved regions in the promoter and 3′ sequence end were manually identified that captured all known promoter and coding sequence mutations. The forward gene specific primer is positions 302 to 320 bp in the SG1 reference MT499781.1 and the

reverse gene specific primer is positions 1495 to1512 bp in the SG1 reference MT499776.1. Primers (Macrogen, Seoul) were tested by running PCR and analysing fragments through gel electrophoresis using genomic DNA from the seven isolates to ensure only one amplicon was present at the correct size. Universal primers and UMI tagging sequences were added to the gene specific primers as in Karst et al.[39]. All primers are listed in Table 2.

DNA extraction and UMI PCR of Cyp51A mock community

To create the *Cyp51A* mock community, DNA was extracted and quantified separately from each of seven *P. teres* isolates and then mixed in equimolar amounts before UMI PCR was performed. UMI PCR, library preparation and sequencing were then performed on the mixed sample. Mycelia from seven *P. teres* isolates was harvested using a scalpel blade from the culture plate, and separately placed in 1.5 mL tubes with two ball bearings and flash frozen in liquid nitrogen. Samples were then ground to a fine powder in a high-speed mixer mill (Retsch MM301, Germany) at 30 rev s^{-1} for one minute. DNA extractions were carried out using the Biosprint 15 DNA Plant Kit and Biosprint 15 robot (Qiagen, Australia) according to the manufacturer's instructions. DNA concentrations were determined on a Qubit Flex Fluorometer using a Qubit dsDNA HS assay kit (Thermo Fisher). Optimal input DNA concentrations for ONT sequencing were calculated to be 1.3 ng based on the 50,000 to 60,000 target strand copies recommended in a similar protocol published by ONT called "Custom PCR UMI" found at https://community.nanoporetech.com/docs/prepare/library_prep_protocols/custom-pcr-umi/v/cpu_9107_v109_revc_09oct2020?devices=minion.

Amplicons tagged with UMIs were generated following Karst et al.[39] and using gene specific and universal primers listed in Table 2. First, a 2117 to 2243 bp region of the *Cyp51A* promoter and coding sequence (Fig. 1) was amplified and tagged with UMIs using GSP_F and GSP_R primers (Table 2). The tagging PCR reaction contained 0.5 µM of each primer, 12.5 µL of 2X Platinum SuperFi II PCR Master Mix (0.08 U μL^{-1},Thermo Fisher Scientific), 1.3 ng of gDNA from each isolate (total of 9.1 ng genomic DNA; Table 1) for a total reaction volume of 25 µL. PCR conditions were as follows: initial denaturation at 95 °C for 3 min followed by 2 cycles of 95 °C for 30 s, annealing at 60 °C for 30 s, followed by final extension at 72 °C for 6 min. The PCR products were purified using AMPure XP beads (Beckman Coulter, California, USA) following manufacturer's instructions except for a 0.6 bead to sample ratio and 80% ethanol concentration. Cleaned PCR products were then dissolved in 10 µL of ultrapure water.

A second PCR was performed using UVP_F and UVP_R (Table 2) to further amplify the UMI-tagged PCR products. The reaction contained 0.5 µM of each primer, 25 µL of 2X Platinum SuperFi II PCR Master Mix and the cleaned UMI-tagging reaction previously described, for a total reaction volume of 50 µL. PCR cycling conditions were as follows: initial denaturation 95 °C for 3 min, followed by 25 cycles of 95 °C for 30 s, annealing at 60 °C for 30 s, 72 °C for 6 min, followed by final extension at 72 °C for 5 min. The resulting PCR products were cleaned using AMPure XP beads (Beckman Coulter, California USA). The purification was performed as described above except for 0.9 bead to sample ratio was used. PCR products were then resuspended in 10 µL of ultrapure water.

To achieve the required number of amplicons for sequencing, a third PCR was carried out with the 20 ng of cleaned PCR products from the second PCR as template, 0.5 µM of primers UVP_F and UVP_R and 50 µL of 2X Platinum SuperFi II PCR Master Mix, in a 100 µL reaction and 11 cycles at the conditions described for the second PCR. PCR products were purified as above for the second PCR and final amplicon concentration measured using a Qubit Flex Fluorometer and Qubit dsDNA HS assay kit (Thermo Fisher Scientific).

ONT sequencing of Cyp51A mock community

Library preparation was carried out using the amplicons from the third PCR reaction and the ONT Ligation Sequencing Kit (SQK-LSK109) following the 'Amplicons by Ligation' protocol as per instructions except for an initial amplicon concentration of 400 fmol. Sequencing was performed on a R10.3 MinION flow cell (FLO-MIN111) and monitored using MinKnow software version 21.02.5. Every 24 h the flow cell was flushed using the ONT Flushing Buffer as per manufacturer instructions and another aliquot of library was loaded to obtain the maximum amount of data. Basecalling was performed using Guppy version 5.0.7 with a minimum q-score of 7. Mutations were validated using qPCR as above.

Culturing of field samples

Five net-blotch symptomatic leaf samples collected in 2021 from barley crops in Minlaton, South Australia, were assessed for fungicide resistance following a culturing method described by Knight et al.[25]. Briefly, infected barley leaves were surface sterilised for 30 s in 70% (v/v) ethanol, 60 s in 0.125% (w/v) NaOCl and 2 × 60 s in autoclaved filtered water, lesions excised, and placed on 2 mL PDA supplemented with streptomycin (10 µg mL^{-1}), ampicillin (100 µg mL^{-1}) and neomycin (50 µg mL^{-1}) dispensed into a 12 well plate. Plates were incubated for seven days at 21 °C in the dark. Resulting fungal growth was scraped from the media and macerated using ball bearings and a mixer mill (Retsch MM400). The mycelial fragments were then distributed onto 24-well plates containing 1 mL PDA with antibiotics as above and either no fungicide, tebuconazole at 15 µg mL^{-1} and 50 µg mL^{-1}, and then incubated at 21 °C in the dark. Fungal growth from each leaf sample was visually assessed after seven days and hyphae growing at both tebuconazole concentrations were harvested.

ONT sequencing of field samples

Genomic DNA of mycelium harvested from both the 15 µg mL^{-1} and 50 µg mL^{-1} tebuconazole wells for each lesion (one lesion per well) were pooled in equimolar amounts and 1.3 ng of each mix was used as template for UMI PCR as described above. Library preparation was carried out using the ONT Ligation Sequencing Kit (SQK-LSK109) following the 'Native barcoding amplicons' protocol as per instructions except for an initial amplicon

concentration of 500 fmol. The five samples were barcoded and sequencing was performed on a R10.3 MinION flow cell (FLO-MIN111) and flushed every 24 h as described above. Basecalling was performed using Guppy version 5.0.12 with a minimum q-score of 7. Mutations were validated using qPCR as above.

Data analysis

Raw passed fastq reads from the five samples were combined and analysed using the longread UMI nanopore pipeline[39] with the following settings: check start of read: 200, check end of read: 200, minimum read length: 2000, maximum read length: 5000, forward adaptor sequence: CAAGCAGAAGACGGCATACGAGAT, forward primer sequence: GCTCGCGTTGGTTGTAGC, reverse adaptor sequence: AATGATACGGCGACCACCGAG ATC, reverse adaptor primer: TTACCGCCTCTCCCAGCA, racon consensus rounds: 2, medaka consensus rounds: 2, medaka model: r103_min_high_g345, bin size cutoff: 10. Maximum read length was chosen due to occasional concatenated sequences, although this made up a relatively small amount of the total sequence data (Supplemental Fig. S3). Consensus sequences from the variants.fa output file were aligned against reference *Cyp51A* sequences using Geneious Prime software version 2021.1.1 (Biomatters Ltd, Auckland New Zealand). For field samples, the five barcodes were pooled for data analysis.

Error rates of UMI consensus sequences were determined by mapping each sequence to its respective reference using Minimap2[46] and calculating the number of errors over the total number of base pairs matched. Chimeras detected using the USEARCH UCHIME2[47] algorithm with the *Cyp51A* reference sequences as the reference library. Scatterplots of read length vs. quality were generated using NanoPlot (https://github.com/wdecoster/NanoPlot).

Quantitative PCR

Quantitative PCR was performed to validate both the mock community and field samples using a magnetic induction cycler (MIC) qPCR system (Bio Molecular Systems, Australia) with two technical replicates per sample. For the mock community, input DNA consisted of an equimolar mix of the seven isolates tested. For the field samples, input DNA was from the pooled 15 µg mL^{-1} and 50 µg mL^{-1} tebuconazole wells for each of the five field samples tested. Positive controls consisted of genomic DNA from the reference isolate known to contain the mutation being tested. Negative controls consisted of genomic DNA from an isolate known not to contain the mutation being tested. Each reaction mixture consisted of 10 uL of ImmoMix™ (Meridian Life Science, USA), 0.25 µM of forward and reverse primers, 0.15 µM of probe and 2.5 ng of template gDNA for a total reaction volume of 20 µL. Assays were developed by Knight et al.[25] and all primers and probes used are listed in Table 2. The cycling conditions were as follows: initial denaturation of 95 °C for 10 min followed by 35 cycles of 95 °C for 15 s and 62 °C for 60 s. Amplification and melt curves were analysed using the micPCR software version 2.10.0 (Bio Molecular Systems). Thresholds were automatically determined using the software and the quantification cycle (Cq) value was determined. A Cq value of less than 35 cycles was considered confirmation of the presence of a particular mutation.

Data availability

Raw amplicon sequence data from the *Cyp51A* mock community and field samples are available at the European Nucleotide Archive under the project number PRJEB64200.

Received: 22 August 2023; Accepted: 11 March 2024
Published online: 15 March 2024

References

1. Kelly, S. L., Arnoldi, A. & Kelly, D. E. Molecular genetic analysis of azole antifungal mode of action. *Biochem. Soc. Trans.* **21**, 1034–1038 (1993).
2. Parker, J. E. *et al.* Resistance to antifungals that target CYP51. *J. Chem. Biol.* **7**, 143–161 (2014).
3. Lamb, D., Kelly, D. & Kelly, S. Molecular aspects of azole antifungal action and resistance. *Drug Resist. Updates* **2**, 390–402 (1999).
4. Cowen, L. E., Sanglard, D., Howard, S. J., Rogers, P. D. & Perlin, D. S. Mechanisms of antifungal drug resistance. *Cold Spring Harb. Perspect. Med.* **5**, a019752 (2014).
5. Cools, H., Hawkins, N. J. & Fraaije, B. Constraints on the evolution of azole resistance in plant pathogenic fungi. *Plant Pathol.* **62**, 36–42 (2013).
6. Cools, H. J. & Fraaije, B. A. Update on mechanisms of azole resistance in *Mycosphaerella graminicola* and implications for future control. *Pest Manag. Sci.* **69**, 150–155 (2013).
7. Becher, R., Weihmann, F., Deising, H. B. & Wirsel, S. G. Development of a novel multiplex DNA microarray for *Fusarium graminearum* and analysis of azole fungicide responses. *BMC Genom.* **12**, 52–69 (2011).
8. Tucker, M. A., Lopez-Ruiz, F., Jayasena, K. W. & Oliver, R. P. *Fungicide Resistance in Plant Pathogens: Principles and a Guide to Practical Management* 329–340 (Springer Japan, 2015).
9. Wyand, R. A. & Brown, J. K. Sequence variation in the *CYP51* gene of *Blumeria graminis* associated with resistance to sterol demethylase inhibiting fungicides. *Fungal Genet. Biol.* **42**, 726–735 (2005).
10. Mair, W. J. *et al.* Demethylase inhibitor fungicide resistance in *Pyrenophora teres* f. sp. *teres* associated with target site modification and inducible overexpression of Cyp51. *Front. Microbiol.* **7**(1279), 1296 (2016).
11. Mair, W. J. *et al.* Parallel evolution of multiple mechanisms for demethylase inhibitor fungicide resistance in the barley pathogen *Pyrenophora teres* f. sp. *maculata*. *Fungal Genet. Biol.* **145**, 103475–103482 (2020).
12. Chamilos, G. & Kontoyiannis, D. P. Update on antifungal drug resistance mechanisms of *Aspergillus fumigatus*. *Drug Resist. Updates* **8**, 344–358 (2005).
13. Fan, J. *et al.* Characterization of the sterol 14α-demethylases of *Fusarium graminearum* identifies a novel genus-specific CYP51 function. *New Phytol.* **198**, 821–835 (2013).
14. Brunner, P. C., Stefansson, T. S., Fountaine, J., Richina, V. & McDonald, B. A. A global analysis of CYP51 diversity and azole sensitivity in *Rhynchosporium commune*. *Phytopathology* **106**, 355–361 (2015).

15. Campbell, G. F., Lucas, J. A. & Crous, P. W. Evidence of recombination between net- and spot-type populations of *Pyrenophora teres* as determined by RAPD analysis. *Mycol. Res.* **106**, 602–608 (2002).
16. Lehmensiek, A. *et al.* Population structure of South African and Australian *Pyrenophora teres* isolates. *Plant Pathol.* **59**, 504–515 (2010).
17. Leišova, L., Minariˇková, V., Kučera, L. & Ovesná, J. Genetic diversity of *Pyrenophora teres* isolates as detected by AFLP analysis. *J. Phytopathol.* **153**, 569–578 (2005).
18. McLean, M. S. *et al.* Validation of a new spot form of net blotch differential set and evidence for hybridisation between the spot and net forms of net blotch in Australia. *Aust. Plant Pathol.* **43**, 223–233 (2014).
19. Turo, C. *et al.* Species hybridisation and clonal expansion as a new fungicide resistance evolutionary mechanism in *Pyrenophora teres* spp. *bioRxiv* **146**, 325 (2021).
20. Fan, F., Yin, W. X., Li, G. Q., Lin, Y. & Luo, C. X. Development of a LAMP method for detecting SDHI fungicide resistance in *Botrytis cinerea*. *Plant Dis.* **102**, 1612–1618 (2018).
21. Duan, Y. *et al.* Development and application of loop-mediated isothermal amplification for detection of the F167Y mutation of carbendazim-resistant isolates in *Fusarium graminearum*. *Sci. Rep.* **4**, 7094 (2014).
22. Zulak, K. G., Cox, B. A., Tucker, M. A., Oliver, R. P. & Lopez-Ruiz, F. J. Improved detection and monitoring of fungicide resistance in *Blumeria graminis* f. sp. *hordei* with high-throughput genotype quantification by digital PCR. *Front. Microbiol.* **9**, 706–716 (2018).
23. Hellin, P. *et al.* Spatio-temporal distribution of DMI and SDHI fungicide resistance of *Zymoseptoria tritici* throughout Europe based on frequencies of key target-site alterations. *Pest Manag. Sci.* **77**, 5576–5588 (2021).
24. Dodhia, K. N., Cox, B. A., Oliver, R. P. & Lopez-Ruiz, F. J. Rapid in situ quantification of the strobilurin resistance mutation G143A in the wheat pathogen *Blumeria graminis* f. sp. *tritici*. *Sci. Rep.* **11**, 4526 (2021).
25. Knight, N., Adhikari, K., Dodhia, K. N., Mair, W. J. & Lopez-Ruiz, F. J. Workflows for detecting fungicide resistance in net form and spot form net blotch pathogens. *bioRxiv* **57**, 151 (2023).
26. Liu, Y.-X. *et al.* A practical guide to amplicon and metagenomic analysis of microbiome data. *Protein Cell* **12**, 315–330 (2021).
27. Schloss, P. D. The effects of alignment quality, distance calculation method, sequence filtering, and region on the analysis of 16S rRNA gene-based studies. *PLoS Comput. Biol.* **6**, e1000844 (2010).
28. Wenger, A. M. *et al.* Accurate circular consensus long-read sequencing improves variant detection and assembly of a human genome. *Nat. Biotechnol.* **37**, 1155–1162 (2019).
29. Earl, J. P. *et al.* Species-level bacterial community profiling of the healthy sinonasal microbiome using Pacific biosciences sequencing of full-length 16S rRNA genes. *Microbiome* **6**, 190 (2018).
30. Samils, B. *et al.* Development of a PacBio long-read sequencing assay for high throughput detection of fungicide resistance in *Zymoseptoria tritici*. *Front. Microbiol.* https://doi.org/10.3389/fmicb.2021.692845 (2021).
31. Gutierrez Vazquez, Y. *et al.* Profiling azole resistant haplotypes within *Zymoseptoria tritici* populations using nanopore sequencing. *Front. Agron.* https://doi.org/10.3389/fagro.2022.943440 (2022).
32. Koren, S. *et al.* Canu: Scalable and accurate long-read assembly via adaptive k-mer weighting and repeat separation. *Genome Res.* **27**, 722–736 (2017).
33. Cherrad, S. *et al.* New insights from short and long reads sequencing to explore cytochrome b variants in *Plasmopara viticola* populations collected from vineyards and related to resistance to complex III inhibitors. *PLoS One* **18**, e0268385 (2023).
34. Wick, R. R., Judd, L. M. & Holt, K. E. Deepbinner: Demultiplexing barcoded Oxford Nanopore reads with deep convolutional neural networks. *PLoS Comput. Biol.* **14**, e1006583 (2018).
35. Kumar, V. *et al.* Long-read amplicon denoising. *Nucleic Acids Res.* **47**, e104 (2019).
36. Hathaway, N. J., Parobek, C. M., Juliano, J. J. & Bailey, J. A. SeekDeep: Single-base resolution de novo clustering for amplicon deep sequencing. *Nucleic Acids Res.* **46**, e21 (2018).
37. Calus, S. T., Ijaz, U. Z. & Pinto, A. J. NanoAmpli-Seq: A workflow for amplicon sequencing for mixed microbial communities on the nanopore sequencing platform. *Gigascience* **7**, 1–16 (2018).
38. Li, C. *et al.* INC-Seq: Accurate single molecule reads using nanopore sequencing. *Gigascience* **5**, 34–45 (2016).
39. Karst, S. M. *et al.* High-accuracy long-read amplicon sequences using unique molecular identifiers with Nanopore or PacBio sequencing. *Nat. Methods* **18**, 165–169 (2021).
40. Marc, A. S. & Patrick, D. S. The impact of DNA polymerase and number of rounds of amplification in PCR on 16S rRNA gene sequence data. *mSphere* **4**, e00163-00119 (2019).
41. Sereika, M. *et al.* Oxford Nanopore R10.4 long-read sequencing enables the generation of near-finished bacterial genomes from pure cultures and metagenomes without short-read or reference polishing. *Nat. Methods* **19**, 823–826 (2022).
42. Radhakrishnan, G. V. *et al.* MARPLE, a point-of-care, strain-level disease diagnostics and surveillance tool for complex fungal pathogens. *BMC Biol.* **17**, 65–82 (2019).
43. Delahaye, C. & Nicolas, J. Sequencing DNA with nanopores: Troubles and biases. *PLoS One* **16**, e0257521 (2021).
44. Inglis, P. W., Pappas, M. C. R., Resende, L. V. & Grattapaglia, D. Fast and inexpensive protocols for consistent extraction of high quality DNA and RNA from challenging plant and fungal samples for high-throughput SNP genotyping and sequencing applications. *PLoS One* **13**, e0206085 (2018).
45. Syme, R. A. *et al.* Transposable element genomic fissuring in *Pyrenophora teres* is associated with genome expansion and dynamics of host–pathogen genetic interactions. *Front. Genet.* https://doi.org/10.3389/fgene.2018.00130 (2018).
46. Li, H. Minimap2: Pairwise alignment for nucleotide sequences. *Bioinformatics* **34**, 3094–3100 (2018).
47. Edgar, R. C., Haas, B. J., Clemente, J. C., Quince, C. & Knight, R. UCHIME improves sensitivity and speed of chimera detection. *Bioinformatics* **27**, 2194–2200 (2011).

Acknowledgements

The authors would like to thank Johannes Debler for help with GPU base calling. This study was supported by the Centre for Crop and Disease Management, a joint initiative of Curtin University, and the Grains Research and Development Corporation – research grant CUR00023.

Author contributions

KZ conceived of the work, performed data analysis, and wrote the manuscript. LFC performed the experiments and contributed to the design of the work. NK created assays used in a qPCR analysis of mock community and field samples. FL contributed to the conception and design of the work. All authors substantively revised the work.

Competing interests

The authors declare no competing interests.

Additional information

Supplementary Information The online version contains supplementary material available at https://doi.org/10.1038/s41598-024-56801-z.

Correspondence and requests for materials should be addressed to K.G.Z.

Reprints and permissions information is available at www.nature.com/reprints.

Publisher's note Springer Nature remains neutral with regard to jurisdictional claims in published maps and institutional affiliations.

Open Access This article is licensed under a Creative Commons Attribution 4.0 International License, which permits use, sharing, adaptation, distribution and reproduction in any medium or format, as long as you give appropriate credit to the original author(s) and the source, provide a link to the Creative Commons licence, and indicate if changes were made. The images or other third party material in this article are included in the article's Creative Commons licence, unless indicated otherwise in a credit line to the material. If material is not included in the article's Creative Commons licence and your intended use is not permitted by statutory regulation or exceeds the permitted use, you will need to obtain permission directly from the copyright holder. To view a copy of this licence, visit http://creativecommons.org/licenses/by/4.0/.

© The Author(s) 2024